

FIG. 2. Perspective drawing of γ N₂ (tetragonal) viewed normal to (110) face showing close packing of prolate molecules.

culated interplanar spacings and reflected intensities for the proposed model of γ N₂. For hcp N₂ at low pressure, the constant B in the Debye-Waller temperature factor has been evaluated⁹ as 1.53 Å². In keeping with the higher density and larger θ_D of tetragonal N₂, we have used the estimated value $B = 1.4$ Å² in computing the expected intensities of Table I.

The structure consists of two types of layers which are perpendicular to the unique axis of the unit cell as shown in Fig. 2. In one of these layers the molecules lie flat in a square array with their long axes parallel and directed along one of the square diagonals. Alternate layers are shift-

ed with the molecules again lying flat and parallel, but with their long axes directed along the other square diagonal and at right angles to molecules in the adjoining layers. This arrangement would seem to minimize the electric-quadrupole-quadrupole energy of the crystal.

A complete treatment of the subject will be submitted to an appropriate journal and will include a discussion of the α and β phases at high pressure and all three phases in nitrogen 15.

*Work performed under the auspices of the U. S. Atomic Energy Commission.

¹C. A. Swenson, *J. Chem. Phys.* **23**, 1963 (1955).

²J. W. Stewart, *J. Phys. Chem. Solids* **1**, 146 (1956).

³We are indebted to T. A. Scott and P. J. Haigh for pointing out to us the need for information about the structure of γ N₂.

⁴*Metals Handbook*, edited by T. Lyman (American Society for Metals, Metals Park, Ohio, 1961), 8th edition, Vol. I.

⁵R. L. Mills and A. F. Schuch, *Phys. Rev. Letters* **6**, 263 (1961).

⁶C. S. Barrett and Lothar Meyer, *Phys. Rev.* **160**, 694 (1967).

⁷R. F. W. Bader, W. H. Henneker, and P. K. Cade, *J. Chem. Phys.* **46**, 3341 (1967).

⁸*International Tables for X-Ray Crystallography*, The International Union of Crystallography, edited by N. F. M. Henry and K. Lonsdale (The Kynoch Press, Birmingham, England, 1952), Vol. I.

⁹W. E. Streib, T. H. Jordan, and W. N. Lipscomb, *J. Chem. Phys.* **37**, 2962 (1962).

OPTICAL DISPERSION AND THE STRUCTURE OF SOLIDS

S. H. Wemple and M. DiDomenico, Jr.

Bell Telephone Laboratories, Murray Hill, New Jersey 07974

(Received 15 September 1969)

A new energy parameter \mathcal{E}_d is introduced to describe dispersion of the electronic dielectric constant. This dispersion energy is found to obey an extraordinarily simple empirical relation in the more than 50 ionic and covalent crystals for which reliable refractive-index dispersion data are available. Based on this result we derive a structure-dependent electronic dielectric response function consisting of constant optical-frequency conductivity with high- and low-frequency cutoffs.

A simple, physically appealing dielectric model of electronegativity and ionicity has been developed recently by Phillips and Van Vechten¹⁻³ using the concepts of homopolar and heteropolar energy gaps. These authors find that a so called "average energy gap" E_g can be computed for a large group of diatomic crystals using simple empirical expressions. This average gap may be decomposed into a homopolar gap E_h and a

heteropolar gap C by the quadrature relation $E_g^2 = E_h^2 + C^2$ and is defined (apart from a factor of order unity) by the equation

$$E_g^2 = (\hbar\omega_p)^2 / [\epsilon_1(0) - 1], \quad (1)$$

where $\hbar\omega_p$ is the plasma energy of the valence electrons, and $\epsilon_1(0)$ is the static electronic dielectric constant ($\epsilon = \epsilon_1 + i\epsilon_2$).

In this Letter we introduce a new energy pa-

parameter \mathcal{E}_d , to describe dispersion of the electronic dielectric constant (or refractive index). This "dispersion energy," which is related to interband transition strengths, obeys an extraordinarily simple empirical relation in over 50 widely different "ionic" and "covalent" nonmetallic crystals. Based on experimental observations we show the following. (1) \mathcal{E}_d is independent of the lowest band gap and internuclear spacing and is essentially the same in all covalent and ionic compounds when normalized by the cation coordination number, anion valency, and number of valence electrons per anion. (2) A realistic model dielectric response function consists of constant optical-frequency conductivity ($\omega\epsilon_2 = \text{constant}$) with high- and low-frequency cut-offs. The dispersion energy is a direct measure of the conductivity. (3) Crystals are found to group into distinct ionic and covalent classes with the transition between the two occurring in AB crystals having the wurtzite structure.

We define the r th moment of the optical spectrum of a crystal by the relation

$$M_r = (2/\pi) \int_{\mathcal{E}_g}^{\infty} \mathcal{E}^{3-2r} \epsilon_2(\mathcal{E}) d\mathcal{E}, \quad (2)$$

where $\mathcal{E} = \hbar\omega$, $\epsilon_2(\mathcal{E})$ is the imaginary part of the electronic dielectric function, and \mathcal{E}_g is the lowest band-gap energy. The real part $\epsilon_1(\mathcal{E})$ is represented by a single Sellmeier oscillator at low energies, i.e.,

$$\epsilon_1(\mathcal{E}) - 1 = \mathcal{F} / (\mathcal{E}_0^2 - \mathcal{E}^2). \quad (3)$$

Here \mathcal{F} and \mathcal{E}_0 are oscillator-strength and interband-energy parameters. As described in detail elsewhere⁴ Eq. (3) is obeyed, for $\mathcal{E} \lesssim \mathcal{E}_g$, in all nonmagnetic materials for which refractive-index dispersion data are available. We emphasize that our use of Eq. (3) does not imply that \mathcal{E}_0 can be identified with any particular interband transition or that only a simplified $\epsilon_2(\mathcal{E})$ spectrum is being considered. It is easy to show⁴ using the Kramers-Kronig (KK) relation that

$$\mathcal{E}_d^2 \equiv (\mathcal{F} / \mathcal{E}_0^2)^2 = M_2^3 / M_3, \quad (4)$$

$$\mathcal{E}_0^2 = M_2 / M_3. \quad (5)$$

We have introduced in Eq. (4) the dispersion energy \mathcal{E}_d , which is defined in such a way as to weight most heavily values of $\epsilon_2(\mathcal{E})$ near the band gap. A relation analogous to Eq. (4) can also be written for the Phillips band-gap parameter E_g defined by Eq. (1). The f -sum-rule integral

$$M_1 = (2/\pi) \int_{\mathcal{E}_g}^{\infty} \mathcal{E} \epsilon_2 d\mathcal{E} = (2/\pi)^2 (\hbar\omega_p)^2, \quad (6)$$

and the KK relation at $\mathcal{E} = 0$, when substituted into Eq. (1), yield the expression

$$E_g^2 = M_1 / M_2. \quad (7)$$

Equation (7) relates E_g to the first and second moments of the ϵ_2 spectrum and thus weights ϵ_2 at higher energies more heavily than the corresponding expression for \mathcal{E}_d . We also note that E_g does not depend on the magnitude of ϵ_2 whereas \mathcal{E}_d does, so that interband transition strengths are not contained in the Phillips-model parameter E_g .

We have fitted refractive-index dispersion data taken from a variety of sources⁴ to Eq. (3) and have obtained the experimental values of \mathcal{F} , \mathcal{E}_0 , and \mathcal{E}_d listed in Table I.⁵ Inspection of Table I shows that \mathcal{E}_d is strikingly constant within the various crystal groupings although \mathcal{F} and \mathcal{E}_0 vary widely. For example $\mathcal{E}_d \approx 12.5$ eV in the NaCl-type alkali halides, and $\mathcal{E}_d \approx 25$ eV in 19 oxides having a variety of complex crystal structures. This factor of 2 difference suggests a possible simple connection between \mathcal{E}_d and the anion valency Z_a . Further support for such a relationship is provided by the ratio 2:3:4 between values of \mathcal{E}_d in II-VI, III-V, and IV-IV compounds. A simple relationship between \mathcal{E}_d and the coordination number N_c of the nearest-neighbor cation is also indicated by Table I. For example a ratio of about 8/6 is observed between 8-coordinated and 6-coordinated halides. Furthermore, all the oxides having values clustering around 25 eV are 6-coordinated despite differences in crystal structure. The two 4-coordinated oxides show values approximately 4/6 as large. The above observations suggest that $\mathcal{E}_d \propto N_c Z_a$. Turning to the thallium halides, we observe that \mathcal{E}_d is somewhat higher than in the isostructural 8-coordinated alkali halides. We believe that the higher oscillator strength in the thallium salts is due to the $6s^2$ electrons of the Tl^+ ion. These two electrons plus the eight electrons in the $s-p$ orbitals would yield a total of $N_e = 10$ valence electrons per anion rather than $N_e = 8$ as in the alkali halides. We might then expect a ratio of 10/8 between corresponding values of \mathcal{E}_d . This is nearly the ratio observed in Table I. The noble-metal salts appear to fall outside the framework outlined above. For example, the value of \mathcal{E}_d in 6-coordinated AgCl is almost a factor of 2 higher than in the isostructural alkali halides, i.e., \mathcal{E}_d is nearly the same as observed in 6-coordinated oxides. Similarly, in zinc-blende CuCl \mathcal{E}_d has almost the same value as observed in 4-coordi-

Table I. Experimentally determined values of the Sellmeier parameters \mathcal{E}_0 and \mathcal{F} , the dispersion energy \mathcal{E}_d , and the normalized dispersion energy $\mathcal{E}_d/N_c Z_a N_e$. For brevity we have included results for only one light-polarization direction in all anisotropic crystals. The various material groupings are labeled according to anion valency Z_a , nearest-neighbor coordination number N_c , and effective number of valence electrons per anion N_e .

| CRYSTAL | $\mathcal{E}_0(\text{eV})$ | $\mathcal{F}(\text{eV}^2)$ | $\mathcal{E}_d(\text{eV})$ | $\mathcal{E}_d/N_c Z_a N_e(\text{eV})$ | CRYSTAL | $\mathcal{E}_0(\text{eV})$ | $\mathcal{F}(\text{eV}^2)$ | $\mathcal{E}_d(\text{eV})$ | $\mathcal{E}_d/N_c Z_a N_e(\text{eV})$ |
|--|----------------------------|----------------------------|----------------------------|--|---|----------------------------|----------------------------|----------------------------|--|
| NaCl-TYPE ($N_c=6, Z_a=1, N_e=8$) | | | | | OXIDES ($N_c=6, Z_a=2, N_e=8$) | | | | |
| LiF | 17.1 | 255 | 14.9 | 0.31 | MgO | 11.3 | 249 | 22 | 0.23 |
| NaF | 15 | 170 | 11.3 | 0.24 | CaO | 9.9 | 224 | 22.6 | 0.24 |
| KF | 14.8 | 183 | 12.3 | 0.26 | Al ₂ O ₃ | 13.4 | 370 | 27.5 | 0.29 |
| NaCl | 10.3 | 141 | 13.6 | 0.28 | Y ₃ Al ₅ O ₁₂ | 11.1 | 282 | 25.4 | 0.26 |
| KCl | 10.5 | 129 | 12.3 | 0.26 | TeO ₂ | 6.24 | 145 | 23.2 | 0.24 |
| RbCl | 10.4 | 127 | 12.2 | 0.25 | SrTiO ₃ | 5.68 | 135 | 23.7 | 0.25 |
| CsCl | 10.6 | 149 | 14.0 | 0.29 | BaTiO ₃ | 5.57 | 131 | 23.3 | 0.24 |
| KBr | 9.2 | 114 | 12.4 | 0.26 | KTaO ₃ | 6.50 | 159 | 23.7 | 0.25 |
| RbBr | 9.1 | 110 | 12.1 | 0.25 | KTO _{0.65} Nb _{0.35} O ₃ | 6.17 | 144 | 23.4 | 0.25 |
| KI | 7.7 | 99 | 12.8 | 0.27 | LiTaO ₃ | 7.49 | 196 | 26.1 | 0.27 |
| RbI | 7.7 | 94 | 12.1 | 0.25 | LiNbO ₃ | 6.65 | 172 | 25.9 | 0.27 |
| CsCl-TYPE ($N_c=8, Z_a=1, N_e=8$) | | | | | Ba₂NaNb₃O₁₅ 6.20 153 24.6 0.26 | | | | |
| CsCl | 10.6 | 181 | 17.1 | 0.27 | TiO ₂ | 5.24 | 135 | 25.7 | 0.27 |
| CsBr | 9.4 | 159 | 17.0 | 0.27 | MgAl ₂ O ₄ | 12.1 | 282 | 23.3 | 0.24 |
| CsI | 7.5 | 114 | 15.2 | 0.24 | CdWO ₄ | 9.15 | 213 | 23.3 | 0.24 |
| CsCl-TYPE ($N_c=8, Z_a=1, N_e=10$) | | | | | ZnWO₄ 7.46 194 26.0 0.27 | | | | |
| TlCl | 5.8 | 120 | 20.6 | 0.26 | CaMoO ₄ | 8.26 | 190 | 23.0 | 0.24 |
| TlBr | 5.3 | 115 | 21.7 | 0.27 | PbMoO ₄ | 5.4 | 122 | 22.6 | 0.24 |
| CaF₂-TYPE ($N_c=8, Z_a=1, N_e=8$) | | | | | SrMoO₄ 8.6 183 21.3 0.22 | | | | |
| CaF ₂ | 15.7 | 249 | 15.9 | 0.25 | OXIDES ($N_c=4, Z_a=2, N_e=8$) | | | | |
| BaF ₂ | 13.8 | 219 | 15.9 | 0.25 | ZnO | 6.4 | 109 | 17.1 | 0.27 |
| NOBLE METAL SALTS ($Z_a=1, N_e=18$) | | | | | SiO ₂ 13.6 250 18.3 0.29 | | | | |
| AgCl ($N_c=6$) | 7.4 | 163 | 22 | 0.20 | ZINC-BLENDE ($N_c=4, Z_a=2, N_e=8$) | | | | |
| CuCl ($N_c=4$) | 7.3 | 132 | 18.1 | 0.25 | ZnS | 6.36 | 164 | 26.1 | 0.41 |
| WURTZITES ($N_c=4, Z_a=2, N_e=8$) | | | | | ZnSe 5.54 150 27.0 0.42 | | | | |
| ZnO | 6.4 | 109 | 17.1 | 0.27 | ZnTe 4.34 117 27.0 0.42 | | | | |
| CdS | 4.9 | 99 | 20.4 | 0.32 | CdTe 4.13 106 25.7 0.40 | | | | |
| CdSe | 4.0 | 82 | 20.6 | 0.32 | ZINC-BLENDE ($N_c=4, Z_a=3, N_e=8$) | | | | |
| ZnS | 6.15 | 155 | 25.2 | 0.39 | GaP | 4.46 | 161 | 36.0 | 0.38 |
| | | | | | GaAs 3.55 119 33.5 0.35 | | | | |
| | | | | | DIAMOND-TYPE ($N_c=4, Z_a=4, N_e=8$) | | | | |
| | | | | | C 10.9 541 49.7 0.39 | | | | |
| | | | | | Si 4.0 178 44.4 0.35 | | | | |
| | | | | | Ge 2.7 110 41 0.32 | | | | |

nated oxides. These results can be understood if the d electrons are included³ in the total N_e , i.e., $N_e \approx 18$ rather than 8.

Based on the experimental results shown in Table I and the observations outlined above we can write the following general empirical expression for \mathcal{E}_d , applicable to over 50 nonmetallic-nonmagnetic compounds containing a single anion species⁶:

$$\mathcal{E}_d = \beta N_c Z_a N_e \text{ eV}, \quad (8)$$

where N_e is the number of effective valence electrons per anion, e.g., $N_e = 8$ in an s - p valence band; $\beta_1 = 0.26 \pm 0.04$ eV for the ionic compounds⁷ (halides and oxides); $\beta_c = 0.39 \pm 0.04$ eV for the covalent compounds⁸ (all nonhalide, zinc-blende, and diamond structures); and β ranges between these extremes in simple AB -wurtzite crystals. The wurtzite structure can thus be viewed as transitional between two well-defined ionic and covalent crystal classes. The transitional character of wurtzites has also been observed experi-

mentally within the dielectric model of Phillips and Van Vechten.² Furthermore, Kurtin, McGill, and Mead⁹ have deduced the existence of distinct ionic and covalent crystal classes based on observations of the barrier energies at metal-semiconductor interfaces, exciton strengths, and the relative importance of "direct" and "nondirect" transitions. These authors also find that wurtzite crystals tend to be distributed near the transition region between ionic and covalent classes. Their results imply, however, that ZnS is nearly ionic whereas we would place this material in the covalent class.

We now propose a dielectric model that can account for the empirical results summarized by Eq. (8). Because \mathcal{E}_d is found experimentally to be independent of the band gap \mathcal{E}_g , a strong constraint is imposed on the form of the fundamental ϵ_2 spectrum [see Eqs. (2) and (4)]. We propose the following simple model ϵ_2 spectrum which satisfies this constraint:

$$\begin{aligned} \mathcal{E}\epsilon_2 &= \sigma\hbar/\epsilon_0, & \mathcal{E}_g < \mathcal{E} < b\mathcal{E}_g, \\ \epsilon_2 &= 0, & \mathcal{E} < \mathcal{E}_g \text{ and } \mathcal{E} > b\mathcal{E}_g. \end{aligned} \quad (9)$$

In Eq. (9) the coefficient b is an arbitrary normalized bandwidth parameter, σ has units of conductivity, and ϵ_0 is the free-space permittivity. Our model dielectric response function thus consists simply of a constant optical-frequency conductivity σ with high- and low-frequency cutoffs. We show this spectrum in Fig. 1 for $b=4$. We also show the single Sellmeier oscillator that produces equivalent dispersion of the refractive index for $\mathcal{E} \lesssim \mathcal{E}_g$. Our model spectrum should be contrasted to the results of the Penn model¹⁰

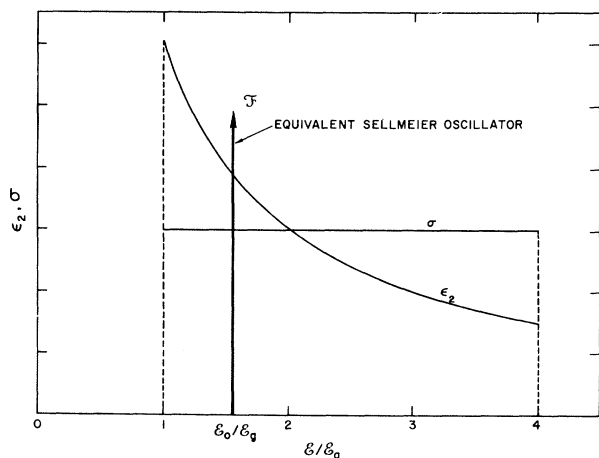


FIG. 1. Model dielectric functions ϵ_2 and σ together with equivalent Sellmeier oscillator for $b=4$.

for which $\mathcal{E}\epsilon_2$ is singular at $\mathcal{E} = \mathcal{E}_g$ and falls off very rapidly with increasing energy.¹¹ Experimentally observed ϵ_2 spectra are more realistically described by the constant- σ model. It is also significant to note that the Penn model gives $\epsilon_1(0)-1 = (\hbar\omega_p)^2/E_g^2$ with no theoretical connection between the parameters $\hbar\omega_p$ and E_g , whereas our model gives $\epsilon_1(0)-1 = \mathcal{E}_d/\mathcal{E}_0$ as a consequence of the observed relation between \mathcal{F} and \mathcal{E}_0 . Structure associated with interband critical points or exciton bands is, of course, generally superimposed on the constant- σ "bond-breaking" background. This structure apparently has little influence on the moment integrals contained in Eq. (4).

Substituting the model spectrum given by Eq. (9) into Eqs. (4), (5), and (7) yields:

$$\mathcal{E}_d = (2\sqrt{3}/\pi)(\hbar/\epsilon_0)\sigma(b-1)/(1+b+b^2)^{1/2}, \quad (10)$$

$$E_g = \sqrt{b}\mathcal{E}_g, \quad (11)$$

$$(\mathcal{E}_0/E_g)^2 = 3b/(1+b+b^2). \quad (12)$$

Therefore in terms of our model the dispersion energy \mathcal{E}_d is a measure of the optical-frequency conductivity σ and is consequently an interband oscillator-strength parameter. The parameter E_g of the Phillips model retains its significance as a band-gap parameter and is simply the geometric mean of the upper and lower cutoff energies. Combining Eqs. (10) and (8) we find that

$$\sigma/N_c Z_a N_e = (\pi/2\sqrt{3})(\epsilon_0/\hbar)\beta(1+b+b^2)^{1/2}/(b-1). \quad (13)$$

Because $\beta_i \approx 0.26$ eV in ionic crystals and $\beta_c \approx 0.39$ eV in covalent crystals, it is tempting to ascribe this difference solely to differences in bandwidth and thus to assign the same universal numerical value to the quantity $\sigma/N_c Z_a N_e$ in all ionic and covalent crystals. In order to estimate the bandwidth parameter we make use of Eqs. (12) and (13) and the following experimental observations: (1) $\beta_c \approx 1.5\beta_i$, and (2) $\mathcal{E}_0 \approx 0.8E_g$ for covalent crystals (compare values of \mathcal{E}_0 shown in Table I with values of E_g tabulated by Van Vechten³). We then find that $b_c \approx 3.4$ and $b_i \approx 2.1$, and, as expected, $b_c > b_i$. Equation (13) now becomes

$$\sigma/N_c Z_a N_e = 80 \pm 12 (\Omega \text{ cm})^{-1}. \quad (14)$$

Equation (14) expresses the striking result that both the magnitude and dispersion of refractive indices in over 50 widely different nonmetallic ionic and covalent crystals can be related to es-

essentially the same normalized value of optical-frequency conductivity. In our model only bandwidth differences distinguish ionic from covalent crystals. Neither the energy gap nor the internuclear spacing enter into the computation of σ . The bandwidth parameters b_c and b_i measure the width of those parts of the conduction and valence bands which play important roles in determining crystal structure. For the more covalent crystals Phillips¹² has correlated crystal structure with a dielectrically defined bond ionicity. Here we have found from a spectroscopic analysis of covalent and ionic crystals that the N_c and Z_a of Pauling's classical resonating-bond theory¹³ play an important role. In both cases the usual picture of crystal structure as determined only by the energies of occupied valence states is discarded in favor of relationships between structure and the optical spectrum.

We wish to thank J. C. Phillips and J. A. Van Vechten for stimulating discussions and helpful comments on the manuscript.

¹J. C. Phillips, Phys. Rev. Letters 20, 550 (1968).

²J. C. Phillips and J. A. Van Vechten, Phys. Rev. Letters 22, 705 (1969).

³J. A. Van Vechten, Phys. Rev. 182, 891 (1969).

⁴S. H. Wemple and M. DiDomenico, Jr., to be published;

for data on some oxides see M. DiDomenico, Jr., and S. H. Wemple, J. Appl. Phys. 40, 720 (1969).

⁵We have excluded from Table I all small-band-gap semiconductors since it is difficult to determine with sufficient accuracy the free-carrier and/or photoionization contribution to the observed refractive-index dispersion for such materials. The results tabulated for Ge may in fact be influenced by such extrinsic effects.

⁶In magnetic transition-metal compounds we would expect weaker oscillator strength for transitions from the occupied d or f orbitals. For example, in EuO $\mathcal{E}_d = 9$ eV rather than approximately 25 eV as observed in 6-coordinated nonmagnetic oxides. In complex crystals containing anion radicals we find, for example, that $\mathcal{E}_d \approx 16$ eV for several phosphates and $\mathcal{E}_d \approx 20$ eV for a group of iodates and carbonates.

⁷Based on available refractive-index data the β values for LiF and AgCl fall slightly outside the limits given for β_i .

⁸The β value for Ge lies slightly below the lower bound given for β_c . This may be due to a small free-carrier contribution to the refractive index data.

⁹S. Kurtin, T. C. McGill, and C. A. Mead, Phys. Rev. Letters 22, 1433 (1969).

¹⁰D. R. Penn, Phys. Rev. 128, 2093 (1962).

¹¹We thank J. A. Van Vechten for providing us with the Penn-model ϵ_2 spectrum.

¹²J. C. Phillips, Chem. Phys. Letters 3, 286 (1969).

¹³L. Pauling, The Nature of the Chemical Bond (Cornell University Press, New York 1960).

REFLECTION SPECTRUM OF SOLID ARGON IN THE VACUUM ULTRAVIOLET*

R. Haensel and G. Keitel

Physikalisches Staatsinstitut, II. Institut für Experimentalphysik der Universität Hamburg, Hamburg, Germany
and

E. E. Koch and M. Skibowski

Sektion Physik der Universität München, München, Germany
and

P. Schreiber

Deutsches Elektronen-Synchrotron, Hamburg, Germany

(Received 13 October 1969)

The reflectance of solid Ar has been measured at 20°K for an angle of incidence of 15° in the photon energy range from 10 to 30 eV using the synchrotron radiation of DESY. The reflectance data reveal a spin-orbit-split exciton series with sharp maxima converging to about 14 eV together with broader peaks above 14 eV due to transitions between the valence and conduction band. The results are compared with the absorption spectrum associated with the $2p$ core levels.

Several optical^{1,2} and electron-energy-loss³ measurements have been performed on solid Ar in order to study its electronic transitions from the valence band. These investigations were confined to the spectral region below 14 eV. They

were made with limited resolution so that the existence of an exciton series converging to the band gap could not clearly be proved. Thus these measurements led to some uncertainty in the determination of the series limit.⁴